JOURNAL OF BACTERIOLOGY, Feb. 1994, p. 702–713
0021-9193/94/$04.00+0

Vol. 176, No. 3

Electric Fields Induce Curved Growth of *Enterobacter cloacae*, *Escherichia coli*, and *Bacillus subtilis* Cells: Implications for Mechanisms of Galvanotropism and Bacterial Growth

ANN M. RAJNICEK,[1,2]* COLIN D. McCAIG,[1] AND NEIL A. R. GOW[2]

Departments of Biomedical Sciences[1] and Molecular and Cell Biology,[2] Marischal College, University of Aberdeen, Aberdeen AB9 1AS, United Kingdom

Received 19 October 1993/Accepted 19 November 1993

Directional growth in response to electric fields (galvanotropism) is known for eukaryotic cells as diverse as fibroblasts, neurons, algae, and fungal hyphae. The mechanism is not understood, but all proposals invoke actin either directly or indirectly. We applied electric fields to bacteria (which are inherently free of actin) to determine whether actin was essential for galvanotropism. Field-treated (but not control) *Enterobacter cloacae* and *Escherichia coli* cells curved rapidly toward the anode. The response was both field strength and pH dependent. The direction of curvature was reversed upon reversal of field polarity. The directional growth was not due to passive bending of the cells or to field-induced gradients of tropic substances in the medium. Field-treated *Bacillus subtilis* cells also curved, but the threshold was much higher than for *E. cloacae* or *E. coli*. Since the curved morphology must reflect spatial differences in the rates of cell wall synthesis and degradation, we looked for regions of active wall growth. Experiments in which the cells were decorated with latex beads revealed that the anode-facing ends of cells grew faster than the cathode-facing ends of the same cells. Inhibitors of cell wall synthesis caused spheroplasts to form on the convex regions of field-treated cells, suggesting that the initial curvature resulted from enhanced growth of cathode-facing regions. Our results indicate that an electric field modulates wall growth spatially and that the mechanism may involve differential stimulation of wall growth in both anode- and cathode-facing regions. Electric fields may therefore serve as valuable tools for studies of bacterial wall growth. Use of specific *E. coli* mutants may allow dissection of the galvanotropic mechanism at the molecular level.

Naturally occurring electric fields exist within and around many single cells and multicellular organisms, including animals, plants, and fungi (10, 32). They result from the polarized distribution of ion channels and pumps within the plasma membrane and may play important roles in processes such as cell guidance and the establishment of cell polarity. Fields of physiologically relevant magnitudes applied in vitro induce changes in cell shape that lead to directional cell growth (galvanotropism), but the mechanisms of the responses remain unknown. All theories invoke actin at some point, usually by suggesting that reorganization of the actin-based cytoskeleton or regional variation in actin assembly-disassembly dynamics dictates cell shape and therefore determines the direction of subsequent growth.

Despite recent evidence that homologs of eukaryotic mechanoproteins exist in bacteria (3, 31), it is generally accepted that bacteria are naturally devoid of actin (22). We have therefore exploited the serendipitous discovery of a galvanotropic bacterium to explore the mechanisms that elicit field-induced directional growth. Although bacteria can swim directionally in response to applied electric fields (1), field-induced changes in the shape of individual cells have not been shown previously for prokaryotes.

Any deviation from normal bacterial morphology must arise from localized alteration in the relative rates of cell wall synthesis and degradation. It would be instructive to consider bacterial galvanotropism in the context of normal growth patterns, but the processes by which bacteria assume and maintain nonspherical shapes during normal cell growth and division are not well understood. In order for the bacterial wall to enlarge, new material must be added to the existing wall that is under considerable tension due to internal hydrostatic pressure. The dilemma of how cells assume nonspherical shapes and grow without bursting has been addressed by the surface stress theory (18, 19, 21, 24). Its basic assumption is that osmotically derived hydrostatic pressure causes tension within the plane of the wall. The wall is not uniformly rigid, and so expansion occurs at regions that are most plastic. Conceptually, growth should be especially problematic for gram-negative bacteria, in which the load-bearing peptidoglycan of the cell wall is extremely thin (19, 23) and the bonds within it are stressed greatly by the cell's high (3 to 5 atm) internal osmotic pressure (20, 21). In the case of gram-negative enteric bacteria, the prevailing form of the surface stress theory is the variable T model, which suggests that cell shape is determined by regional variation of T, the analog of surface tension (23). Although new murein is inserted all over the surface of gram-negative rods (30), localized variations in T lead to regional differences in the bond stresses within the sacculus, which in turn dictate the rate of cell wall growth. Growth is slow where T is high (at the old poles and on the side walls) and is faster where T is lower (at the developing division sites).

This study illustrates that bacteria curve as they grow in applied electric fields. Our data suggest that this striking morphology arises from field-induced regional variation in wall growth rates on the anode- and cathode-facing sides of cells. The ability to manipulate T locally may therefore be a valuable tool in the effort to understand the process of normal growth. Our data also imply that the mechanism for galvanotropism is not the same for all cell types. Specifically, actin is not an

* Corresponding author. Mailing address: Department of Biomedical Sciences, Marischal College, University of Aberdeen, Aberdeen AB9 1AS, United Kingdom.

essential component of the mechanism, at least for prokaryotic cells.

MATERIALS AND METHODS

Cell culture. The majority of this work utilized an organism isolated fortuitously as a contaminant exhibiting marked galvanotropism. A sample of the organism was sent to the National Collections of Industrial and Marine Bacteria, Ltd. (Aberdeen, Scotland), where it was found to most closely resemble *Enterobacter cloacae* on the basis of classic biochemical tests (National Collections of Industrial and Marine Bacteria reference no. ID 2392/NCID 508). The isolate was atypical of *E. cloacae* (35), however, in having a positive methyl red test and a negative Voges-Proskauer test. We refer to this isolate hereafter as *E. cloacae*. Cells were grown in a shaking incubator overnight at 30°C in nutrient broth for *E. cloacae* and *Bacillus subtilis* (University of Aberdeen Culture Collection no. 483) or LB broth for *Escherichia coli* (strain DH5α) and were transferred to 2% (wt/vol) malt extract medium buffered with 20 mM sodium phosphate (pH 7.0) for 1 h prior to the experiment. The media were purchased from Oxoid, Basingstoke, Hampshire, England. All experiments were carried out in 2% (wt/vol) malt extract medium because its high resistivity (909 Ω · cm at 30°C) reduced the current required to achieve the desired voltages. The 20 mM sodium phosphate proved sufficient to buffer the inevitable pH changes at the electrodes.

Growth inhibitors and antibiotics. All antibiotics were purchased from Sigma Chemical Co. (St. Louis, Mo.). Cephalexin promotes filamentation by inhibiting penicillin-binding protein 3 (PBP3), which is involved in septum formation (41). Nalidixic acid inhibits DNA gyrase, thus preventing cell division but not cell elongation. Chloramphenicol, tetracycline, and kanamycin were each used to inhibit protein synthesis. Penicillin G and D-cycloserine were used to inhibit cell wall synthesis. Stock solutions of antibiotics were prepared in normal malt extract medium (unless specified otherwise) at the following concentrations: 5 mg/ml for cephalexin, 35 mg/ml for chloramphenicol (in ethanol), 10 mg/ml for tetracycline, 5 mg/ml for nalidixic acid, 10 mg/ml for kanamycin, 10 mg/ml for D-cycloserine (in malt extract medium, pH 8.0), and 150,000 U/ml for penicillin G (in malt extract medium with 0.15 M $MgSO_4$). Working concentrations of these compounds are presented in Tables 2 and 3.

Electric field application. Electric fields were applied to cells growing on microscope slides (5). Glass microscope slides were treated with 0.1% (wt/vol) poly-L-lysine (Sigma Chemical Co., St. Louis, Mo.) for 30 min, rinsed with distilled water, and allowed to air dry. Cell suspensions were allowed to settle onto the slides for 30 min before they were rinsed gently with malt extract medium and placed onto the gel tray of a standard Bio-Rad electrophoresis mini-sub cell. A peristaltic pump was used to perfuse medium through the chamber continuously (380 ml/min) to disrupt any gradients (e.g., pH) formed around the electrodes. To control field-induced resistive heating, the circulating medium was passed through a water-jacketed cooling coil to maintain a constant 28°C. Temperature and pH were monitored at 30-min intervals and were adjusted if necessary, but the conditions were generally stable during a standard 4-h experiment. For a sample of 10 experiments, the mean temperature (± standard deviation) was 27.9 ± 1.2°C and the mean pH (± standard deviation) was 6.97 ± 0.04. Control cultures were also grown in electrophoresis cells with perfusion. Since the chambers were not connected to the power supply, they were kept in a water bath to maintain the medium at 28°C. Perfusion of medium did not affect the straight morphology of control cells (see Fig. 2); therefore, control slides were sometimes maintained in an incubator (in medium-filled petri dishes).

Cells were fixed by immersing the slides in 10% formalin (Sigma Chemical Co., St. Louis, Mo.) at various intervals after field initiation and were mounted permanently by using drops of DPX (BDH Ltd., Poole, England). Data were quantitated directly from DPX-mounted slides (see below).

Time lapse observations of growing cells. Electric field chambers for time lapse observation were similar to those described previously for use with animal cells (37). They were constructed from Falcon plastic tissue culture dishes (100 by 20 mm). Two strips of glass (a standard microscope slide cut lengthwise or 64-mm-long strips of no. 1 coverglass) were secured with silicone sealant to the dish bottom parallel to each other and 1 cm apart, thus creating a central trough for cell growth. The trough was filled with 0.1% poly-L-lysine for 30 min, rinsed with distilled water, and allowed to air dry. The cell suspension was allowed to settle onto the base of the chamber for 15 to 30 min at 32°C. The dish was then rinsed gently with distilled water to remove loosely adherent cells, and sufficient malt extract medium was added to fill the trough. The medium was filtered (0.2-μm pores) prior to use in all time lapse experiments to improve its optical clarity. A 4.0-cm-long glass coverslip was secured with silicone grease to the two glass spacers, thus creating the chamber roof. Strips of paper towel saturated with distilled water were placed inside each dish to inhibit evaporation. Electrical contact to the chamber was made via two 20-cm-long U-shaped agar bridges (2% [wt/vol] agar dissolved in 2% malt extract medium). One end of each bridge rested in a pool of medium continuous with that in the central trough, and the other end of each bridge terminated in a saline-filled beaker containing a Ag-AgCl electrode. The electrodes were connected to a direct-current constant-voltage electrophoresis power supply (Consort Bioblock). This arrangement prevented contamination of the culture medium by electrode products. In some cases, phenol red was added to the electrode baths and agar bridges to monitor field-induced pH changes. Although pH changes were observed within the electrode baths, there was never a detectable pH shift in the region of the agar bridge near the chamber.

Time-lapse recordings were made of the cells (total magnification, ×132), using a Panasonic video camera mounted on a Nikon Diaphot inverted phase-contrast microscope. During observation, the chamber was maintained at 32°C by an incubator (Nikon) that surrounded the microscope stage. Recordings were made onto S-VHS videotape, using a Panasonic AG-6720 time-lapse video recorder, and images were analyzed from recordings by using an Argus-10 image processor (Hammamatsu Photonics, Hammamatsu, Japan) that allowed further fourfold enlargement of the image.

Cells decorated with latex beads. Cells were labeled with latex beads to monitor the relative growth rates of the ends of single cells. A bead on each cell was used as a reference marker for measurement of the bead to tip distance at 5-min intervals. A suspension of 0.5-μm-diameter plain latex microspheres (Polysciences, Inc., Warrington, Pa.) or a suspension of the same beads coated with poly-L-lysine (42) was added to a liquid culture of *E. cloacae*. There was no apparent difference in the ability of plain or polylysine-treated beads to adhere to cells, and there was no difference in the growth rates for cells with or without beads (data not shown). Suspensions of decorated cells were incubated at 32°C for about 15 min, and then an aliquot was placed into a field chamber. Fresh medium was perfused through the chamber after 10 min to dislodge weakly adherent

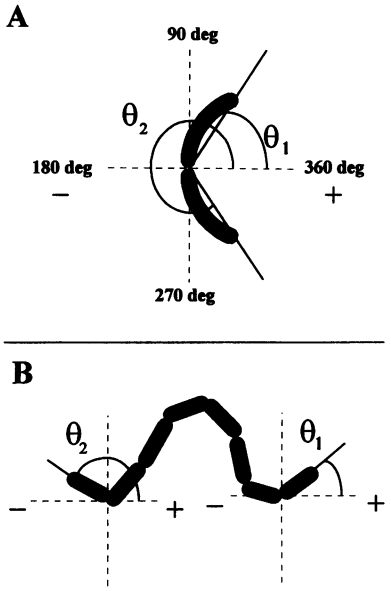

FIG. 1. Angle measurement protocol for determining the percent polarization for a population of bacteria. (A) Data only for doublets of *E. cloacae* or *E. coli* cells that had not separated completely. Angles were measured relative to the cathode/anode axis, with the cathode at 180° and the anode at 360°. See Materials and Methods for calculation of percent polarization. When filamentation was induced in *E. cloacae* by treatment with cephalexin or nalidixic acid, the angles were measured from the cell center to each apex rather than from the point where two cells touched. (B) Data for the terminal cells of chains (with at least eight cells) of *B. subtilis*.

cells and to wash out stray beads. The cultures were then exposed to fields and videotaped as described above.

Average cell extension rates (micrometers per minute) were calculated by measuring the bead-to-tip distance over a time interval and dividing the change in length by the duration of the interval. For cells decorated with more than one bead, distances and angles were measured from the bead nearest the cell center. Cell ends were grouped according to their orientation at the beginning of observation. They were categorized relative to the cathode/anode axis as cathode-facing (or left for control intervals; 180 ± 45°), anode-facing (or right for control intervals; 360 ± 45°), pointing up (90 ± 45°), or pointing down (270 ± 45°).

Electron microscopy. Cells were cultured in field chambers as described above except that they were grown on a 1-cm^2 piece of poly-L-lysine-coated glass used as the roof of the chamber. Cells were fixed for 2 h in 2.5% glutaraldehyde with 2.5 mM $MgCl_2$ and 0.89 M sodium phosphate buffer (pH 7.2). Cells were postfixed in OsO_4, dehydrated, critical point dried in CO_2, and mounted for electron microscopy as described previously (41). Cell diameters were measured directly from the photographic negatives by projecting the image from an enlarger.

Quantifying the field response. Data for cells grown in electrophoresis chambers were quantified directly from DPX-mounted slides viewed with an Olympus TMD phase-contrast microscope. The image was sent from a video camera to a monitor interfaced with a BBC Master microcomputer (11). Data collection was restricted to doublets of cells that had divided but had not separated completely at the end of 4 h of field exposure (Fig. 1A). These were thought to represent cells growing actively during electric field treatment. Since *B. subtilis* often grew as chains of cells, data were also collected from the terminal cell at each end of a chain containing at least eight cells (Fig. 1B). This analysis confirmed that cells in chains responded in the same way as isolated doublets; therefore, we report only data for doublets. A mouse was used to draw a line connecting the point at which the two cells adjoined each other to the distal tip of each cell. In cases in which cells were treated with cephalexin or nalidixic acid, the line was drawn from the center of the cell rather than from the point where two cells joined. The angle (θ) of each line relative to the field direction (cathode at 180°; anode at 360°) was measured, and the percent polarization (29) was calculated as $[(\Sigma \cos \theta)/n] \cdot 100$. Values of 100, −100, and 0% indicate maximum anodal, cathodal, and no orientation, respectively.

Time-lapse data were analyzed from video recordings, using an image processor that allowed further enlargement of the image (total magnification, ×528) and direct measurement of cell lengths (at 5-min intervals) on the monitor. Outlines of the cells were traced from the monitor onto acetate sheets, and angle measurements were made by hand for each cell at 5-min intervals. Angles of growth for each end of a cell were determined by connecting the center of the cell to the tip of each end of the cell. All statistical comparisons were made by using a Student's two-tailed *t* test unless specified otherwise.

RESULTS

Qualitative description of field responses. *E. cloacae* and *E. coli* cells exposed to electric fields often grew through dramatic arcs with the open end of the curve (concave side) facing the anode (Fig. 2D and E). In contrast, control cells maintained their usual straight, rod shapes (Fig. 2A and B). Time-lapse observations confirmed that individual cells curved anodally as they grew (Fig. 3), so that the convex side faced cathodally. Curved cells then divided, each daughter cell continuing to bend until it divided again. After several hours, a confluent layer of curved cells developed.

The curving was not due to selective adhesion to the substratum. Cells became concave anodally even if the ends of growing cells were not attached to the polylysine-coated surface. Additionally, cells that detached spontaneously from the growth surface retained their curved shapes as they floated freely in the liquid medium. To determine whether electric field treatment altered the shape of the cell wall per se, we isolated sacculi by immersing the slides (with field-treated cells attached) briefly in boiling 4% sodium dodecyl sulfate. Using phase-contrast microscopy, we found that most of the cells detached from the slide following this treatment, but the floating cells retained their curved morphology. The dramatic loss of image contrast for floating cells relative to those still adhering to the slide suggested that the detached cells had been lysed effectively.

Quantitative description of directional growth. Field-treated cells exhibited a variety of curved morphologies, ranging from slight bends to unevenly curved J shapes to symmetrical U shapes (e.g., Fig. 2 and 5). Cells were monitored during field exposure to determine whether this variation reflected the orientation of the cells at the beginning of field exposure (i.e., are ends of cells already parallel to the cathode/anode axis less prone to field-induced bending than perpendicular ones?). Quantitation of the galvanotropic response was complicated by cell division, so for most time lapse experiments, *E. cloacae* was treated with cephalexin, which induces filamentation (38). This treatment permitted observation of both ends of a single cell over a long period. The degree of field-induced curvature for each end of a cell was determined with respect to the cathode/anode axis of the field. A tip was considered to deflect if it

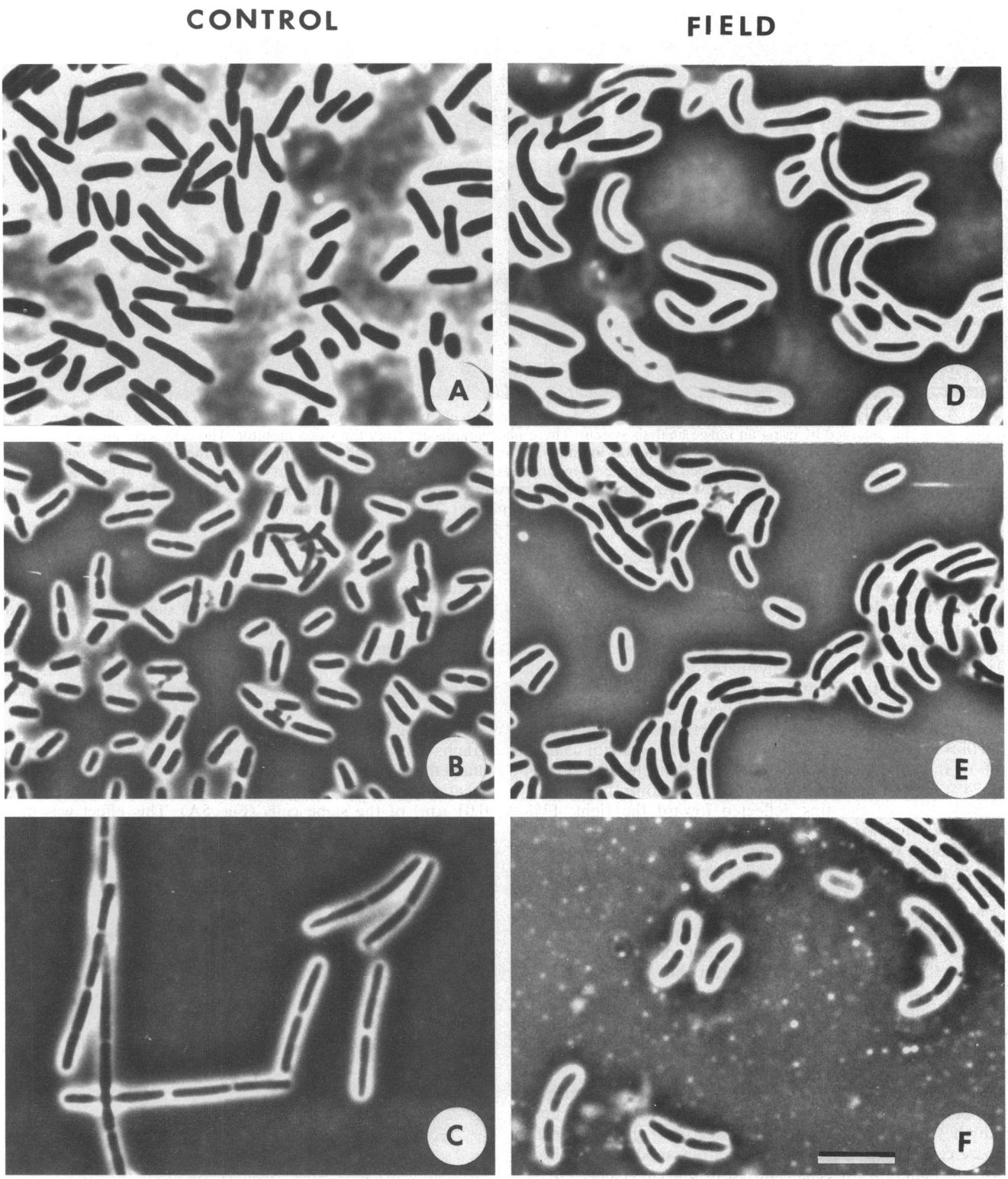

FIG. 2. Phase-contrast micrographs of bacteria growing for 4 h on polylysine-coated microscope slides. (A to C) *E. coli* (A), *E. cloacae* (B), and *B. subtilis* (C) in the absence of a field; (D) *E. coli* exposed to a field of 15 V/cm; (E) *E. cloacae* exposed to a field of 15 V/cm; (F) *B. subtilis* exposed to an electric field of 25 V/cm. The anode is to the right for all photographs of field-treated cells. The scale bar represents 5 μm for all photographs.

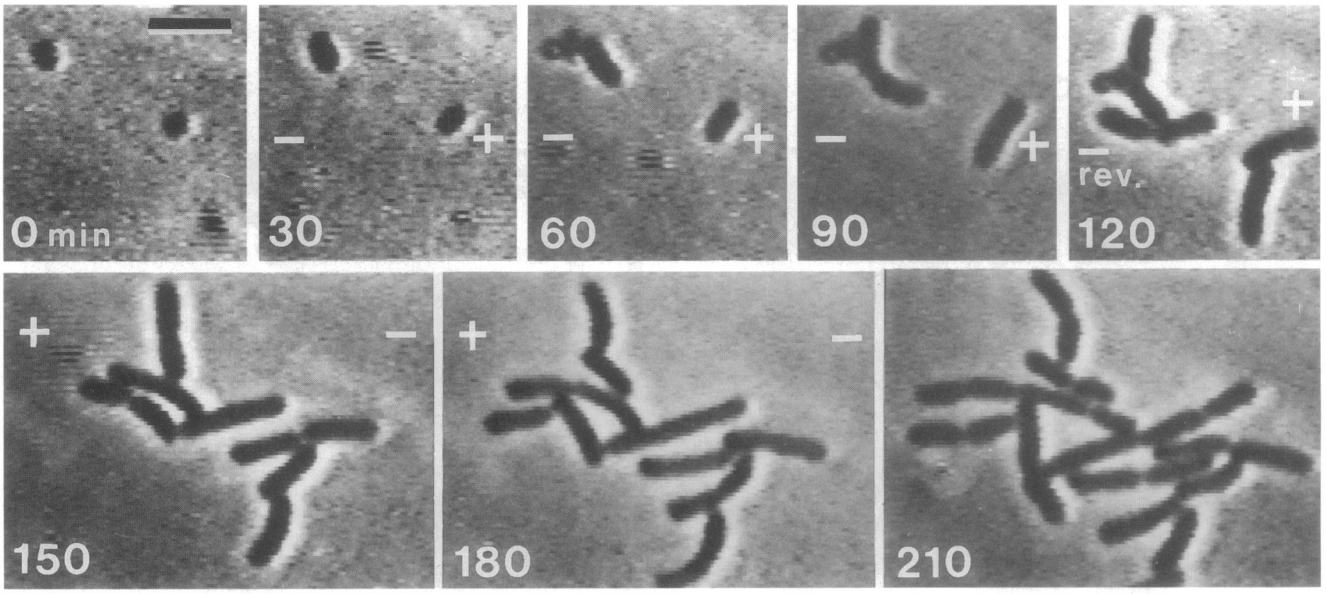

FIG. 3. Individual *E. cloacae* cells growing in the presence and absence of an electric field. Phase-contrast images of growing cells were recorded on videotape and enlarged by using an image analysis system. These photographs are from the video monitor. The cells were grown for 30 min in the absence of a field, and then a field of 14 V/cm was initiated at t = 30 min, with the cathode to the left and the anode to the right of each photograph. Individual cells curved and divided during the 90-min field exposure. The polarity of the field was reversed (rev.) at t = 120 min. The cells responded toward the new anode by reversing their direction of curvature. The field was switched off at t = 180 min. During the subsequent 30 min, individual cells reverted to their relatively straight rod-like morphology. The scale bar represents 5 μm for all frames.

deviated from its original angle by 10° or more during field exposure. This value was chosen because although they did not bend preferentially toward either end of the growth chamber, the cephalexin-treated control cells grew to be very long (up to 50 μm) and followed slightly wavy paths, varying their angles of growth by an average of 10°.

The tips of field-treated cells deflected toward the anode, but control cells did not alter their direction of growth. For 83 cells (n = 166 tips) exposed to fields of 8 to 12 V/cm for 45 min, 74% of the tips deflected anodally, 2% deflected cathodally, and 24% did not deflect. In contrast, for 31 control cells (n = 62 tips), 13% of the tips deflected toward the right, 13% deflected toward the left, and 74% did not deflect.

The initial orientation of the cell determined the field-induced morphology. Ends of cells oriented within 15° of the anode at field initiation continued growing toward the anode during field exposure (mean deflection ± standard error of the mean [SEM], 1.9 ± 2.1° [n = 13]). In contrast, tips growing within 15° of perpendicular (n = 19) deflected an average of 34.6 ± 5.1° anodally, and tips growing within 15° of the future cathode (n = 14) deflected 17.4 ± 5.6° anodally. The relatively large deflection for cathode-facing tips compared with that for anode-facing tips reflects the fact that cathodally oriented tips would have to turn through angles as large as 180° to grow anodally.

Threshold field strength for directional growth. The magnitude of the directional response was dependent on field strength (Fig. 4). There was no directional growth for *E. cloacae* cells in the absence of a field, but anodal galvanotropism was apparent for cells exposed to 2 V/cm ($0.005 < P < 0.01$; one-tailed Student's t test), the lowest field tested. Curved growth was also evident during time-lapse observations of *E. cloacae* (no cephalexin) exposed to 3.3 V/cm for 75 min, which confirmed that the threshold value was 3.3 V/cm or less. Between 5 and 20 V/cm, the magnitude of the response increased with increasing field strength. Polarization was maximal in response to 25 V/cm but fell off slightly at higher fields (Fig. 4). The shape of the field strength dependence curve for *E. coli* was similar to that for *E. cloacae*, including a threshold at 2 V/cm ($0.005 < P < 0.01$; one-tailed Student's t test), but the maximum response was observed between 15 and 20 V/cm, after which there was a slight decline (Fig. 4).

Scanning electron microscopy. Scanning electron micrographs of cephalexin-treated *E. cloacae* revealed that the mean diameter (n = 16) of anode-facing ends (0.88 ± 0.02 μm) was greater ($P < 0.001$) than that of cathode-facing ends (0.68 ± 0.01 μm) of the same cells (Fig. 5A). This effect was most striking for cells growing parallel to the field, perhaps because

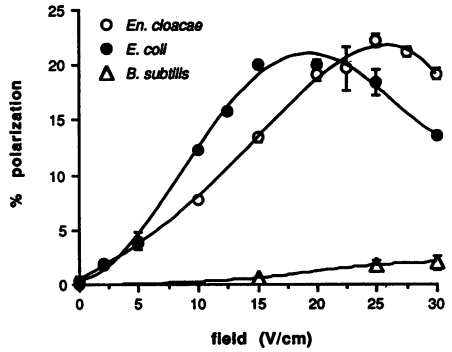

FIG. 4. The directional growth response is dependent on field strength. The percent polarization was calculated by using the equation presented in Materials and Methods. Each point represents the mean for 600 cells (three samples of 200 cells each); error bars (SEM) are an indication of sample-to-sample variability. Error bars do not appear when they are smaller than the symbol.

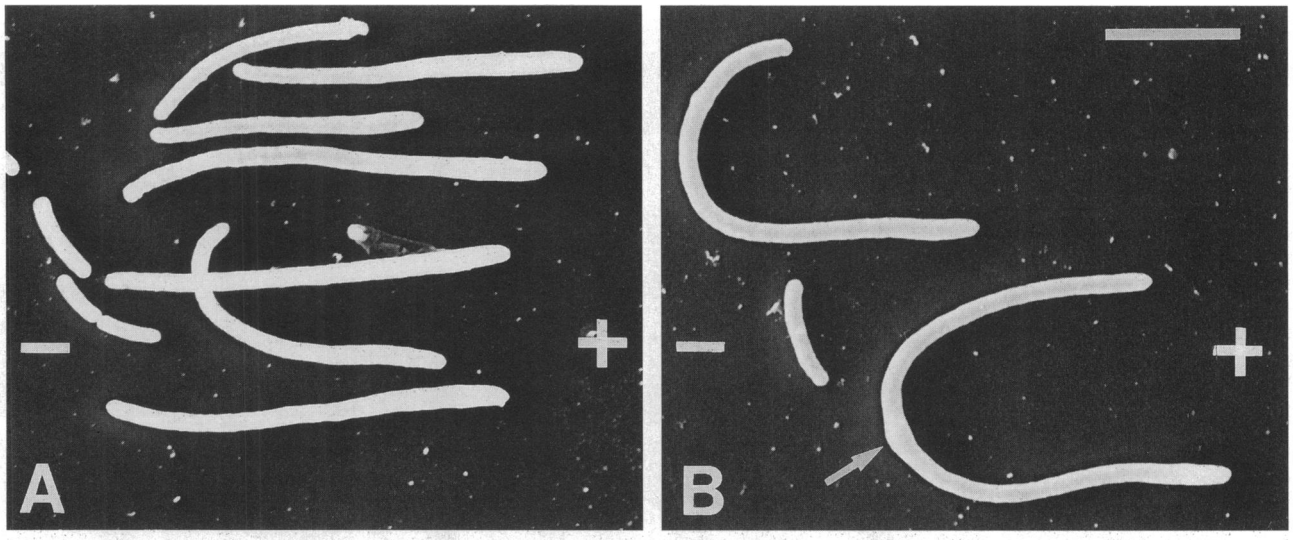

FIG. 5. Scanning electron micrographs of cephalexin-treated *E. cloacae* cells exposed to 16 V/cm for 2 h. (A) The straight cells in this photograph were probably parallel to the field direction when the field was initiated. Note that the anode-facing halves of the cells (to the right) are swollen compared with the cathode-facing halves of the same cells. (B) Cells that are concave toward the anode (right). The arrow indicates the bulge often observed on cephalexin-treated cells. The scale bar represents 5 μm for both photographs.

in a uniform electric field they would experience a larger voltage drop along their length than cells perpendicular to the field would experience across their diameter. The cell surface appeared relatively smooth, but some cephalexin-treated cells showed localized bulges (Fig. 5B). These were also observed by phase-contrast microscopy during time-lapse observation of cephalexin-treated cells. Similar bulges have been reported at the presumptive site of septum formation in cephalexin-treated *E. coli* cells (38).

Field effects on growth of *B. subtilis*. The morphology of *B. subtilis* cells growing in a field of 15 V/cm for 4 h was the same as that of control cells ($0.1 > P > 0.05$; one-tailed Student's *t* test), but the cells did respond to fields 25 or 30 V/cm (Fig. 2 and 4). At these field strengths, the cells were curved but their orientation was not as uniform as for *E. cloacae* or *E. coli* (Fig. 2F). As a result, the percent polarization was small but significantly higher ($0.025 > P > 0.01$; one-tailed Student's *t* test) than for the control populations. The threshold field strength required to elicit a response was therefore about 10-fold higher than that for *E. cloacae* or *E. coli*.

The absence of a response at lower field strengths was confirmed by time-lapse video microscopy. Because *B. subtilis* cells were active and often swam away during the early stages of observation, they were secured to the polylysine-coated surface with an overlay of malt extract gelled with 1% agarose. Individual *B. subtilis* cells grew and divided (4 of the 14 cells had divided once by the end of field treatment), but they did not exhibit a directional response. After 30 min in a field of 12 V/cm, the percent polarization was 1.1 ± 65.1 ($n = 18$). The error value is high because of the low number of cells in the visual field and because the cells retained their random orientation throughout the experiment. Since *E. coli* cells grown beneath a layer of 1% agarose retained the ability to curve anodally (data not shown), the absence of a response for *B. subtilis* is not an artifact of the overlay method.

Effect of reversal of field polarity and termination of the field. When the field polarity was reversed after the initial exposure, *E. cloacae* cells responded rapidly by reversing the direction of curvature so that the cell became concave toward the new anode (Fig. 3 and 6). This was a continuous process by which cells became progressively less curved and straightened momentarily during their transition to oppositely directed growth. This occurred whether the cells were treated with cephalexin (Fig. 6A) or not (Fig. 3).

The degree of curvature became gradually less after the field was switched off (Fig. 3). The cells continued to grow and divide, eventually becoming straight rods again. This was most evident for rapidly dividing cells not treated with cephalexin. Cephalexin-treated cells showed responses ranging from rapid relaxation of curvature to maintenance of its curved shape as the cell grew.

Field effects on elongation rates. Elongation rates were determined by measuring the length of cephalexin-treated *E. cloacae* cells directly from time-lapse videotaped images. Each cell was measured at the beginning and end of a 15-min interval (no field) and over the subsequent 45-min field exposure (or 45-min control interval). The difference in length for each cell was divided by the time interval to yield an average extension rate. There was no difference ($P > 0.5$) between the extension rates for cells prior to field application; cells destined for field exposure ($n = 83$) and control cells ($n = 30$) elongated at a rate (mean ± SEM) of 0.06 ± 0.01 μm/min. Cells from both populations grew faster during the subsequent 45-min interval (probably because the cells had been released from stationary phase), but field-treated cells elongated significantly ($P < 0.001$) faster (0.21 ± 0.01 μm/min; $n = 83$) than their control counterparts (0.12 ± 0.01 μm/min; $n = 30$).

The enhanced extension rate for field-treated cells could be a direct effect of the field on elongation rates of anode-facing versus cathode-facing sides of individual cells. Alternatively, it could be an indirect effect of the field via resistive heating of the growth medium. To distinguish between these possibilities, field-induced heating of the growth medium was monitored with a surface temperature probe placed directly on the coverglass roof of the field chamber. Fields of 9 to 15 V/cm (approximately the fields used for the growth experiments) caused a reversible 3.0 to 3.5°C rise in the medium temperature relative to the ambient temperature (32°C), but this

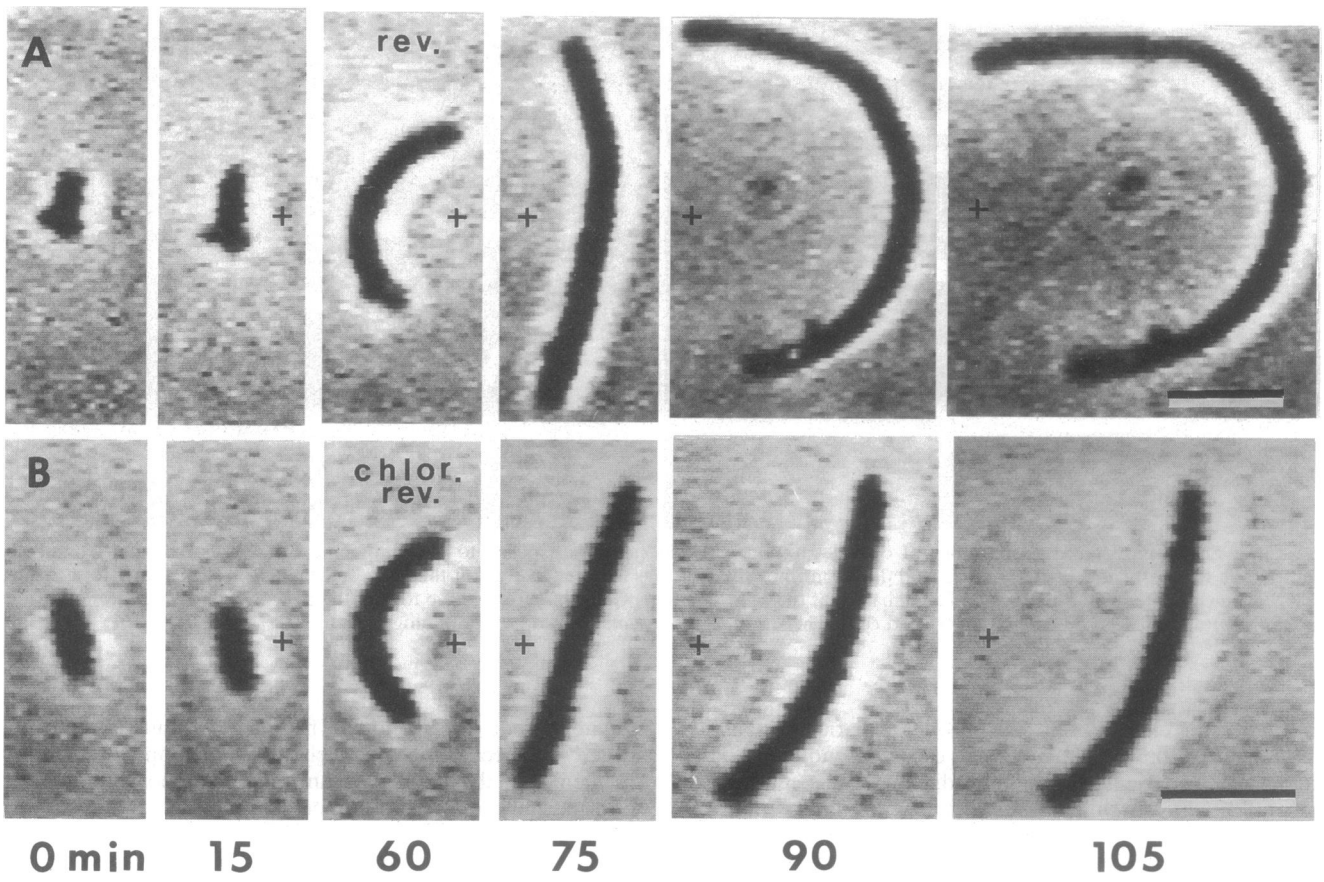

FIG. 6. Time-lapse photographs of cephalexin-treated *E. cloacae* cells exposed to an electric field. Photographs are from the video monitor. (A) The cell was grown for 15 min in the absence of a field. A field of 11.5 V/cm was initiated at t = 15 min, with the cathode to the left of the photographs and the anode to the right. The cell became concave anodally during the subsequent 45 min. At t = 60 min, the field polarity was reversed (rev.) (the anode was now to the left). (B) The conditions were identical to those for panel A except that the field strength was 10 V/cm and chloramphenicol (chlor.) was added to the medium at the time of field reversal (t = 60 min). The cell continued to elongate and reverse its direction of growth for a period despite the presence of chloramphenicol. Note that no new growth or curving is evident between t = 90 min and t = 105 min. This cell's elongation and turning responses are presented graphically in Fig. 9. The scale bar represents 5 μm for all frames.

amount of heating did not account for the enhanced growth rate. Elongation rates were determined for control cells that were grown at 32°C for 15 min and were then raised to 35°C for the next 45 min. These values were compared with the elongation rates reported above for cells maintained at 32°C continuously. The elongation rate at 32°C (0.06 ± 0.02; n = 14) was the same ($0.5 < P < 0.9$) during the initial 15 min as that found previously for cells at that temperature, and the growth rate (0.13 ± 0.01; n = 14) after the shift to 35°C for 45 min was not different ($0.5 < P < 0.9$) from that for control cells maintained at 32°C continuously. Elongation of field-treated cells was significantly faster than for controls during the 45-min interval at either 32°C ($P < 0.001$) or 35°C ($0.001 < P < 0.01$). Field-induced resistive heating was, therefore, not sufficient to explain field-enhanced rates of cell elongation.

Cells were decorated with latex beads to determine whether the increased elongation rate was due to a selective increase in the extension rate of anode-facing regions versus cathode-facing regions of individual cephalexin-treated cells (Table 1). The cell extension rate was the same for both ends of cells regardless of orientation during the 15-min control interval. During field exposure, there was no difference in the rate of growth for ends of cells oriented perpendicular to the field (up compared with down), but the anode-facing ends of cells grew more rapidly than the cathode-facing ends of the same cells (Table 1 and Fig. 7).

There was also an increase in the elongation rate for ends of cephalexin-treated cells growing directly toward the anode

TABLE 1. Influence of an electric field (8 to 12 V/cm) on the elongation rate of *E. cloacae* cells treated with cephalexin

Orientation of tip relative to bead[a]	Mean elongation rate (μm/min) ± SEM	
	Control cells (n)	Field-treated cells (n)
Up	0.07 ± 0.01 (10)	0.09 ± 0.02 (14)
Down	0.07 ± 0.01 (10)	0.10 ± 0.02 (14)
Cathode-facing	NA[b] (0)	0.08 ± 0.02 (15)
Anode-facing	NA (0)	0.14 ± 0.03[c] (15)
Cells without beads	0.11 ± 0.02 (21)	0.21 ± 0.01[d] (53)

[a] Orientation of each end of the cell measured from the latex marker bead. For control cells, tips pointing up or left were pooled together, as were those pointing down or right.

[b] NA, not available because data for control cells were pooled as described in footnote *a*.

[c] Faster than the cathode-facing ends of the same cells ($0.01 < P < 0.025$, one-tailed Student's t test).

[d] Increase compared with control cells without beads ($P < 0.001$).

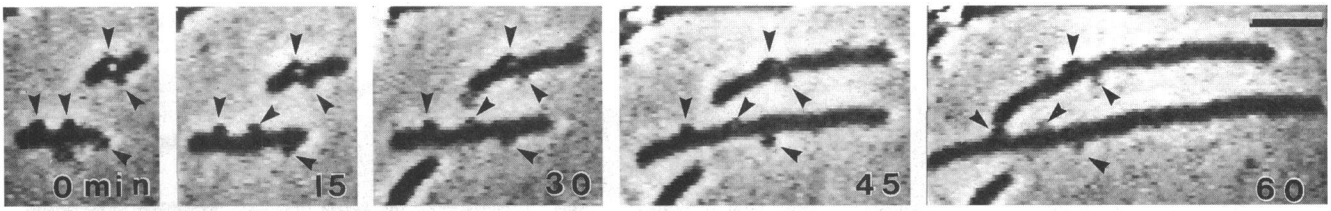

FIG. 7. *E. cloacae* cells decorated with latex beads showing enhanced rates of growth toward the anode. The photographs are from the video monitor. The cells were allowed to grow for 15 min before the field was initiated. The cells were then exposed to 8 V/cm continuously between 15 and 60 min (anode to the right of the photographs). Positions of the latex beads are indicated by the arrowheads. Note that both cells show increased rates of anodal growth relative to the cathode-facing ends of the same cells. The scale bar represents 5 μm for all frames.

(either because they were maintaining their prefield anodal orientation or because they had turned to grow anodally) compared with ends of cells not growing anodally. Anodally directed cell tips elongated at a rate of 0.14 ± 0.02 μm/min (n = 24), but those growing in all other directions grew at 0.07 ± 0.01 (n = 34; $P < 0.001$).

These experiments also suggested that for cells roughly perpendicular to the field, curved growth results from enhanced wall growth on the cathodal sides of cells compared with the anodal sides. Two of the cells monitored continuously retained four beads (one pair on the anode-facing and one pair on the cathode-facing side) throughout field exposure. The mean rate (± standard deviation) at which the two beads on the same side of the cell (i.e., future convex or concave side) moved apart was measured as the cells curved in fields. Beads on the convex (cathodal) sides of cells moved apart more rapidly (0.08 ± 0.02 μm/min) than beads on the concave (anodal) sides of the same cells (0.05 ± 0.01 μm/min; $0.05 > P > 0.025$ by a one-tailed Student's t test).

Treatment of gram-negative bacteria with high levels of penicillin causes localized wall rupture and formation of an osmotically stable spheroplast at that site (7, 39). Since the site of spheroplast formation is thought to represent the actively growing region of the wall (39), we applied penicillin G to field-treated *E. cloacae* cells (in the presence of cephalexin) to test the notion that curvature of cells results from locally enhanced cathodal growth. Time-lapse observation confirmed that elongation ceased immediately upon addition of 1,500 U of penicillin G per ml (cells were resistant to 100 or 600 U/ml). Spheroplasts formed on 87 to 89% of the cells after a mean lag time of 19.6 ± 2.4 (mean ± SEM) min. The positions of the spheroplasts relative to the field direction are summarized in Table 2. The majority (77 to 81%) of spheroplasts formed on the convex (cathode-facing) sides of curved cells (Fig. 8). This was not an artifact of filamentation because the same was true for cells in the absence of cephalexin (Table 2). There was no evident cathode/anode bias of spheroplast sites for cells aligned parallel to the field, but in the absence of cephalexin, there was an increase in the number at the center of the cells. This is probably because it was difficult to detect significant bias on the very short cells. Spheroplast formation on the convex sides of cells was not a peculiar response to penicillin because for cephalexin-treated cells, spheroplasts formed at the same positions upon addition of D-cycloserine, another cell wall synthesis inhibitor (Table 2).

Effects of inhibitors of protein synthesis or cell division on directional growth. The directional growth response was not due to passive bending of the cells. *E. cloacae* cells did not curve in response to fields of 15 V/cm when growth was inhibited by tetracycline, kanamycin, or chloramphenicol, antibiotics that prevent protein synthesis (Table 3). Growth curves (measured at an optical density of 600 nm) for cells in the same media confirmed that each antibiotic suppressed growth of *E. cloacae* effectively. Galvanotropism was not prevented by inhibition of septum formation with use of cephalexin or by inhibition of DNA synthesis with use of nalidixic acid (Table 3). The cells grew as long filaments that became concave anodally (e.g., Fig. 6A).

Chloramphenicol was added to the medium during time-lapse observation to determine whether there was a correlation between field-induced curvature and extension rate. The drug was added after 45 min of field exposure. In some experiments, the polarity of the field was reversed at the time of chloramphenicol addition to assist detection of inhibition of bending. The results were similar regardless of field polarity. Chloramphenicol (50 or 100 μg/ml) inhibited cell growth after an initial lag of 23.3 ± 1.5 min (n = 49) and inhibited turning after 19.0 ± 2.7 min (range, 5 to 40 min; n = 24). Cessation of growth inhibited further curving of the cells (Fig. 6B and 9). Cells sometimes stopped turning before they stopped elongating, but the reverse situation was never observed. The lag time for the effect was not related to cephalexin treatment because

TABLE 2. Site of spheroplast formation relative to the electric field direction[a]

Antibiotic (concn)	Cephalexin concn (μg/ml)	Cells parallel to field				Cells curved anodally			Total no. of cells
		Mean % ± SEM			n	Mean % ± SEM		n	
		Cathode-facing	Center	Anode-facing		Convex	Concave		
Penicillin G (1,500 U/ml)	0	21 ± 4	55 ± 4[b]	24 ± 5	151	65 ± 2[c]	35 ± 3	385	600
	50	35 ± 3	38 ± 7	26 ± 4	216	77 ± 5[c]	23 ± 5	827	1,200
D-Cycloserine (200 or 300 μg/ml)	50	42 ± 15	36 ± 8	22 ± 5	278	81 ± 4[c]	19 ± 1	798	1,200

[a] Cells exposed to fields of between 9 and 12 V/cm were scored as populations of 200 cells. Data for cells without cephalexin represent three sets of 200 cells. Data for cephalexin-treated cells represent six sets of 200 cells. D-Cycloserine data include one experiment at 200 μg/ml and one at 300 μg/ml (both at pH 8.0 because cycloserine is unstable at neutral or acid pH). Statistical significance was determined by a two-tailed Student's t test.

[b] Different from percent cathode-facing ($P < 0.001$) or percent anode-facing ($0.01 < P < 0.001$).

[c] Greater than the percent with spheroplasts on the concave side ($P < 0.001$).

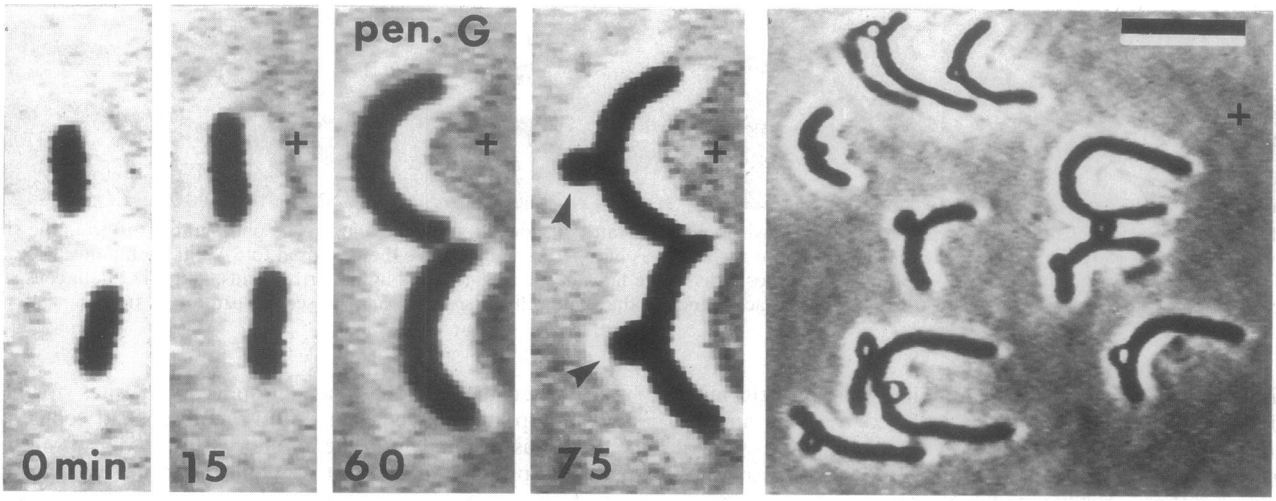

FIG. 8. Time-lapse photographs of cephalexin-treated *E. cloacae* showing spheroplast formation on the convex sides of curved cells. The photographs are from the video monitor. Cells were allowed to grow for 15 min prior to field initiation. After 45 min in a field of 9 V/cm (T = 60), 1,500 U of penicillin G per ml was added. Spheroplasts (at arrowheads) formed in the center of the convex sides of both cells within 15 min. The cells retained their curved shapes even after wall rupture, which would drastically reduce the cell's normally high internal osmotic pressure. This suggests that the shape of the cell wall has been altered by the field. The final photograph shows other cells in the same dish 25 min after penicillin G addition. Spheroplasts are usually found on the convex regions of curved cells. The scale bar represents 5 μm for the first four frames and 10 μm for the final frame.

there was a similar delay for cells never exposed to cephalexin. It was clear, therefore, that there was a temporal correlation between growth and bending such that the cells could grow without bending, but they could not bend without growing. We conclude from these data that galvanotropism requires de novo protein synthesis. The lag period for cessation of growth and turning probably represents the depletion of a cellular pool of proteins required for directional growth.

Influence of extracellular pH. The magnitude of the electric field response depends on the pH of the growth medium. *E. cloacae* cells were grown in malt extract medium with McIlvaine's Na_2HPO_4-citric acid buffer ranging in pH from 5.5 to 8.0. The magnitude of the response increased with increasing pH (Fig. 10), with a maximum at pH 7.5 followed by a slight decline. A similar increase at pH 7.5 was observed with use of 20 mM sodium phosphate buffer over a pH range of 6.5 to 7.5 (data not shown). Measurements of optical density at 600 nm for cells growing in media with McIlvaine's buffer indicated that the doubling time (1.2 h) was identical for cells at pH 6, 7, or 8, but it was extended slightly (1.6 h) at pH 5. Regardless of extracellular pH, all cultures entered log phase within 2.5 h, which is well within the 4-h duration of the directional growth assay. The effect of pH on directional growth is therefore not simply due to pH-induced variation in growth rates.

TABLE 3. Influences of inhibitors of protein synthesis, DNA synthesis, and septum formation on field-induced curvature of *E. cloacae*

Inhibitor	Concn (μg/ml)	Target	% Polarization ± SEM[a]
None		None	13.4 ± 0.4
Chloramphenicol	75	Peptidyltransferase	1.2 ± 0.2
Tetracycline	25	Aminoacyl-tRNA	1.2 ± 0.0
Kanamycin	50	30S ribosome subunit	0.7 ± 0.5
Cephalexin	50	PBP3	20.2 ± 1.2
Nalidixic acid	20	DNA gyrase subunit A	24.8 ± 1.6

[a] Each value represents the mean of three sets of 200 angle measurements each. See Fig. 1 and Materials and Methods for angle measurement protocol. Polarization for control cultures ranged from 0.3% ± 0.4% (no inhibitor) to 0.9% ± 0.5% (nalidixic acid). These near-zero values indicate a lack of directional growth.

DISCUSSION

Our data indicate that bacteria are galvanotropic despite their lack of actin, high internal osmotic pressure, and fairly rigid cell wall. Several observations confirmed that the bending

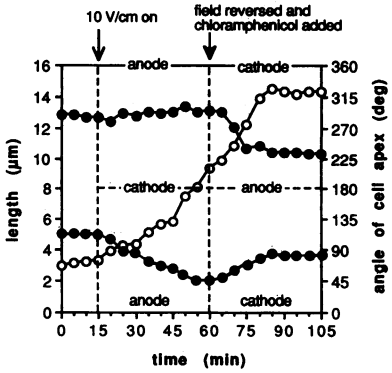

FIG. 9. Chloramphenicol-induced cessation of growth is correlated temporally with inhibition of orientation. The graph represents the length (open circles) and the orientation of each apex (closed circles) of the cephalexin-treated cell in Fig. 6B. The field was applied for 45 min, with the cathode at 180° and the anode at 360 (0)°. At t = 60 min, the field polarity was reversed and chloramphenicol was added to the medium. Both ends of the cell turned in response to the field (although one end turned more during the initial exposure). When the field polarity was reversed, both ends of the cell turned toward the new anode. The cell continued to elongate for 25 min before the chloramphenicol prevented cell elongation. The lag times for the inhibitory effect of chloramphenicol on turning were 15 min for one end of the cell and 25 min for the other.

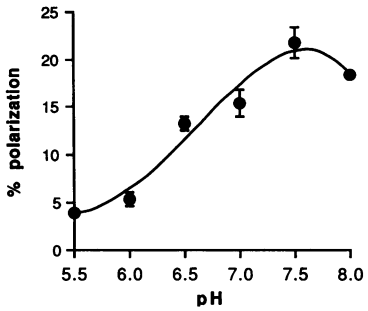

FIG. 10. The magnitude of the directional response is dependent on the pH of the growth medium. Each point represents the mean of three populations of 200 measurements each. *E. cloacae* cells were grown in malt extract medium with McIlvaine's buffer while exposed to fields of 15 V/cm for 4 h. Control cells grown in the same media in the absence of a field did not show a field response (i.e., percent polarization = 0). Cells did not grow well outside the pH range indicated here. Error bars represent SEM.

of these cells was a response to the electric field and was not induced by other experimental conditions. For example, the curved morphology was not the result of selective adhesion of one side of the elongating cell to the substrate because field-treated cells retained their curved shapes after dislodging spontaneously from the substrate and because the ends of cells not attached to surfaces also curved anodally as they grew. Curved growth did not result from electro-osmotic water flow at the polylysine-coated (positively charged) growth surface because field-treated *E. cloacae* cells also became concave anodally on untreated (negatively charged) glass or plastic surfaces. Constant perfusion of medium through the chambers ensured that curved growth was not due to field-induced gradients of tropic factors (e.g., pH) in the medium. Perfusion itself did not induce curvature because (i) curved growth was not affected by the direction of perfusion (anode toward cathode or vice versa), (ii) perfusion did not induce curvature of cells never exposed to fields, and (iii) the response was observed when electrical field chambers that lacked a perfusion pump and that were well isolated from the electrodes (to protect growing bacteria from electrode products) were used.

The finding that bacteria alter their shapes rapidly and reversibly in response to applied electric fields has implications for the mechanism of bacterial wall synthesis and the general mechanism of electric field-induced directional growth. There are several theories for how animal cells sense and respond directionally to small extracellular voltage gradients (38). For example, an applied field perturbs the membrane potential so that cells are hyperpolarized on their anode-facing sides and depolarized on their cathodal sides (2, 12). This regional perturbation affects the inward-driving force for ions locally and alters the probability that voltage-gated channels for ions such as Ca^{2+} would be open. Electric field-induced Ca^{2+} influx results in spatially localized gradients of Ca^{2+} within animal cells that would affect the local dynamics of actin microfilament assembly and disassembly in a way that could lead to directional growth (2, 6). A similar mechanism may operate in fungi (10, 26).

The actin-based cytoskeleton is the major shape-determining component of animal cells, but the cell wall performs this role in bacteria (20, 22). This difference suggests that although the effect on cytoskeletal structure may be appropriate for galvanotropic animal cells, it is not relevant for bacteria, which lack microfilaments. Our data confirm that the shape of the cell wall is altered by the applied field. The field's effect must therefore stem from localized variation in T, which affects wall structure or rate of synthesis locally.

Bacterial wall growth is a complex process that involves a delicate balance between murein synthesis and hydrolysis (13). The gross morphological changes that we observed must therefore result from a shift in this balance such that it favors net synthesis in a particular region. Two lines of evidence support this idea. (i) The anode-facing ends of cells grew more rapidly than the cathode-facing ends. This was apparent both from the swelling of the anodal tips of cells relative to the cathodal tips of the same cells and from direct measurement of growth rates of the ends of cells labeled with latex beads. (ii) Spheroplasts formed mainly on the convex side of field-treated cells. We measured the rates of growth of convex versus concave sides of cells as they grew in fields in an attempt to demonstrate that cathodal spheroplast formation was not merely the result of lateral tension in the convex wall. In the few cells meeting the stringent selection criteria, beads on the convex (cathodal) sides of cells moved apart more rapidly than those on the concave (anodal) sides of the same cells. Taken together, these results suggest that a cell roughly perpendicular to the field grows more rapidly on its cathode-facing side, which causes the cell to become concave anodally.

As mentioned previously, external electric fields modulate membrane potential (2, 12). How could this difference in membrane potential across the cell be translated into asymmetric wall growth? One possibility consistent with the variable T model for gram-negative cells is that the transcellular difference in membrane potential alters the ionic conductance of the membrane, causing localized ion currents. For example, if proton pumps are more active in a specific region of the cell, the pH and zeta potential would be altered locally and the free energy of the transpeptidation reaction may thereby be influenced (23). We cannot determine directly whether membrane potential perturbation plays a role in bacterial galvanotropism because technical limitations make it impossible to resolve regional differences in the membrane potential within a single bacterium. This mechanism remains feasible, however, because extracellular electric fields of 0.1 to 1.0 mV/μm perturb the membrane potential of mouse neuroblastoma cells significantly (2), and our data indicate that *E. cloacae* and *E. coli* cells respond to fields as low as 2.0 V/cm, which corresponds to a potential difference across the cell (assuming a 1-μm diameter) of 0.20 mV. Interestingly, the galvanotropic response threshold for gram-negative bacterial cells is the same as that for animal cells, on the order of 0.1 mV per cell diameter (36). In the case of gram-positive bacteria, changes in membrane potential might affect the activity of wall-degrading enzymes. Autolytic enzymes, which control cell wall thickness, are sensitive to both the electrical and pH gradients across the membrane (16, 17).

In what other way might an electric field induce asymmetric growth? It might induce a physical redistribution of the cellular machinery responsible for cell wall synthesis, resulting in locally enhanced rates of wall growth. One way in which this could occur is by electric field-induced redistribution of proteins within the plane of the membrane via lateral electrophoresis (14) or electro-osmosis (29). This phenomenon has been demonstrated directly for eukaryotes (33, 34) and is thought to be the most likely mechanism for galvanotropism of animal cells (36) and fungal hyphae (9, 27). Our finding that the magnitude of the galvanotropic response of bacteria depends on the extracellular pH is consistent with observations of field-treated fungal hyphae in which the magnitude and in some cases the polarity of the galvanotropic response is

determined by the pH of the growth medium (9, 26). The net charge of membrane-bound proteins would become more negative with increasing pH; therefore, the correlation between increasing pH and increasing galvanotropism suggests that galvanotropism is mediated by a direct electrophoretic anodal redistribution of membrane-bound proteins. Spherical myoblasts exposed to fields of 1 to 10 V/cm show an obvious anode/cathode asymmetry in the distribution of receptor proteins within 5 min of field initiation (33). The effective fields used in the present study were generally within that range, but the diameter of the cells was about 20 times smaller, which may explain why we observed bacterial galvanotropism as early as 3 min after field initiation for rapidly growing cells. When the field is switched off, growing cells revert gradually to their normal straight rod-like morphology, suggesting that postfield back diffusion eventually restores the prefield uniform orientation of membrane proteins and diffuse wall growth. Postfield relaxation has been shown for concanavalin A receptors (33, 34) and for epidermal growth factor receptors (8) in animal cells.

The targets for redistribution in bacteria are not necessarily membrane-bound proteins, but potential candidates must be (i) accessible to the electric field, (ii) mobile within the cytoplasm, cell membrane, periplasm, or outer membrane (for gram-negative bacteria), and (iii) involved in the establishment or maintenance of cell shape by affecting wall biosynthesis either directly or indirectly. Which cellular constituents meet these requirements? Cytoplasmic components were once excluded as candidates for field-induced redistribution on theoretical grounds because the plasma membrane should insulate the cell interior from most of the externally applied field (15). There is recent evidence, however, that charged molecules migrate electrophoretically through the cytoplasm of cells exposed to extracellular electric fields (4) and that larger cytoplasmic components such as yolk granules, actin filaments, and ribosomes accumulate anodally within cells (27). We have preliminary evidence that bacterial DNA is distributed asymmetrically in field-treated bacteria (34a); therefore, it would be interesting to determine whether a cytoplasmic asymmetry of other cellular components (such as ribosomes) is induced in bacteria by externally applied electric fields.

So far, we can only speculate on the possible targets for electrophoretic redistribution, but for gram-negative cells, the outer membrane proteins are likely candidates because their extracellular regions would be readily accessible to the field. Evidence that outer membrane proteins (porins) are voltage sensitive (25) makes them attractive targets even if they are not redistributed within the plane of the membrane.

Our data for locally enhanced wall growth present a conundrum. How can a uniform electric field stimulate both anodal and cathodal rates of wall synthesis in the same cell? One possibility is that there are two separate mechanisms responsible for field-induced curvature, one acting at the anode-facing tips of cells and the other acting on the cathodal sides of cells. For a cell that is roughly perpendicular to the field, we hypothesize that the initial curvature results from cathodal stimulation of wall growth (perhaps via events triggered by cathodal depolarization of the membrane) and that once the cell begins to bend, a second mechanism (anodal electrophoresis) comes into play. These separate mechanisms may be invoked by a single cell in a uniform field if the processes have different response thresholds. For example, the region of a cell perpendicular to a field would experience a smaller voltage drop across its diameter than curved regions of the same cell would (Fig. 11). As a result, the voltage drop would be larger for regions that were curved and would continue to increase as the end of the cell became increasingly parallel to the field. The voltage drop would be maximal when the ends of the cell were exactly parallel to the field, perhaps explaining why the cells do not become C or O shaped. If the threshold (voltage drop per micrometer) was smaller for the cathode-stimulated mechanism (depolarization) than for the anode-stimulated mechanism (electrophoresis), the geometry of the situation would result in regional differences in the mechanism employed. This dual mechanism proposal is consistent with our data for localized wall growth and the pH dependence of galvanotropism.

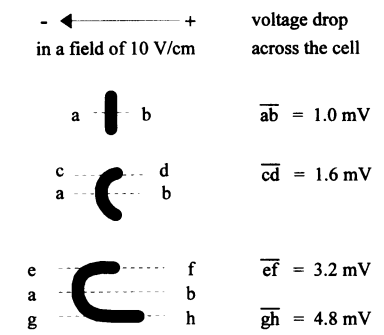

FIG. 11. Hypothetical mechanism for bacterial galvanotropism. A 1-μm-diameter cell that is oriented perpendicular to an applied field of 10 V/cm experiences a voltage drop of 1.0 mV across itself (ab). For regions of cells beginning to curve in response to the field (cd), the transcellular voltage drop increases and continues to increase as the ends of the cell grow anodally (ef). The regional transcellular potential is maximal for ends of the cell growing exactly parallel to the field (gh). The voltage drop across the center of the U shape (ab) remains constant throughout the process. The resulting regional differences in transcellular potential are translated by the cell into curved growth. We suggest that where the voltage difference is minimal (ab), growth is stimulated cathodally, perhaps by depolarization of the cathode-facing membrane. As the voltage drop increases (cd, ef, and gh), another mechanism (perhaps anodal electrophoresis of cell wall-synthesizing machinery) is triggered that requires a larger transcellular voltage difference for activation. The transcellular voltage differences beside each drawing were determined directly from measurements of the relative diameters of the cell in this drawing at the electric field lines indicated by the broken lines.

We acknowledge that the conditions used for these experiments are artificial; bacteria would not usually experience a voltage gradient of several volts per centimeter in their natural environments. This does not diminish the significance of this novel observation, however. The ability to manipulate the process of wall growth locally has tremendous potential as a tool for understanding the mechanism of bacterial shape determination. The use of specific *E. coli* mutants will allow dissection of the molecular basis for polarized cell wall growth, perhaps also providing insight into the mechanism for eukaryotic galvanotropism. This molecular approach was impractical previously with most galvanotropic cells. Further experiments using cells grown in defined media will characterize the ionic requirements for bacterial galvanotropism and extend the survey of susceptible bacterial types.

ACKNOWLEDGMENTS

We thank David Gregory and Debbie Marshall for help with the scanning electron micrographs. We are also grateful to Frank Harold, Ian Booth, and Mike Morris for stimulating discussions and comments on the manuscript.

This work was funded by The Wellcome Trust.

REFERENCES

1. **Adler, J., and W. Shi.** 1988. Galvanotaxis in bacteria. Cold Spring Harbor Symp. Quant. Biol. **53**:23–25.
2. **Bedlack, R. S., Jr., M.-D. Wei, and L. M. Loew.** 1992. Localized membrane depolarizations and localized calcium influx during electric field-guided neurite growth. Neuron **9**:393–403.
3. **Casaregola, S., V. Norris, M. Goldberg, and I. B. Holland.** 1990. Identification of a 180 kD protein in *Escherichia coli* related to a yeast heavy-chain myosin. Mol. Microbiol. **4**:505–511.
4. **Cooper, M. S., J. P. Miller, and S. E. Fraser.** 1989. Electrophoretic repatterning of charged cytoplasmic molecules within tissues coupled by gap junctions by externally applied electric fields. Dev. Biol. **132**:179–188.
5. **Crombie, T., N. A. R. Gow, and G. W. Gooday.** 1990. Influence of applied electrical fields on yeast and hyphal growth of *Candida albicans*. J. Gen. Microbiol. **136**:311–317.
6. **Davenport, R. W., and S. B. Kater.** 1992. Local increases in intracellular calcium elicit local filopodial responses in helisoma neuronal growth cones. Neuron **9**:405–416.
7. **Donachie, W. D., and K. J. Begg.** 1970. Growth of the bacterial cell. Nature (London) **227**:1220–1224.
8. **Giugni, T. D., D. L. Braslau, and H. T. Haigler.** 1986. Electric field-induced redistribution and postfield relaxation of epidermal growth factor receptors on A431 cells. J. Cell Biol. **104**:1291–1297.
9. **Gooday, G. W., and N. A. R. Gow.** Shape determination and polarity in fungal cells. *In* D. Ingraham (ed.), Shape and form in plant and fungal cells, in press. Academic Press, London.
10. **Gow, N. A. R.** 1989. Circulating ion currents in microorganisms. Adv. Microb. Physiol. **30**:89–123.
11. **Gray, D. I., and B. M. Morris.** 1992. A low cost video analysis system for the BBC Master computer. Binary **4**:58–61.
12. **Gross, D., L. M. Loew, and W. W. Webb.** 1986. Optical imaging of cell membrane potential changes induced by applied fields. Biophys. J. **50**:339–348.
13. **Höltje, J.-V., and U. Schwarz.** 1985. Biosynthesis and growth of the murein sacculus, p. 77–119. *In* N. Nanninga (ed.), Molecular cytology of *Escherichia coli*. Academic Press, London.
14. **Jaffe, L. F.** 1977. Electrophoresis along cell membranes. Nature (London) **265**:600–602.
15. **Jaffe, L. F., and R. Nuccitelli.** 1977. Electrical controls of development. Annu. Rev. Biophys. Bioeng. **6**:445–476.
16. **Jolliffe, L. K., R. J. Doyle, and U. N. Streips.** 1981. The energized membrane and cellular autolysis in *Bacillus subtilis*. Cell **25**:753–763.
17. **Kirchener, G., A. L. Koch, and R. J. Doyle.** 1984. Energized membrane regulates cell pole formation in *Bacillus subtilis*. FEMS Microbiol. Lett. **24**:143–147.
18. **Koch, A.** 1983. The surface stress theory of microbial morphogenesis. Adv. Microb. Physiol. **24**:301–366.
19. **Koch, A. L.** 1984. How bacteria get their shapes: the surface stress theory. Comments Mol. Cell. Biophys. **2**:179–196.
20. **Koch, A. L.** 1985. Bacterial wall growth and division or life without actin. Trends Biochem. Sci. **(January)**:11–14.
21. **Koch, A. L.** 1985. How bacteria grow and divide in spite of internal hydrostatic pressure. Can. J. Microbiol. **31**:1071–1084.
22. **Koch, A. L.** 1991. The wall of bacteria serves the roles that mechano-proteins do in eukaryotes. FEMS Microbiol. Rev. **88**:15–26.
23. **Koch, A., and I. D. J. Burdett.** 1984. The variable *T* model for Gram-negative morphology. J. Gen. Microbiol. **130**:2325–2338.
24. **Koch, A. L., M. L. Higgins, and R. J. Doyle.** 1982. The role of surface stress in the morphology of microbes. J. Gen. Microbiol. **128**:927–945.
25. **Lakey, J. H., and F. Pattus.** 1989. The voltage-dependent activity of *Escherichia coli* porins in different planar bilayer reconstitutions. Eur. J. Biochem. **186**:303–308.
26. **Lever, M., B. Robertson, A. Buchan, P. F. P. Miller, G. W. Gooday, and N. A. R. Gow.** pH and Ca^{2+} dependent galvanotropism of filamentous fungi: implications and mechanisms. Mycol. Res., in press.
27. **McCaig, C. D., and P. J. Dover.** 1991. Factors influencing perpendicular elongation of embryonic frog muscle cells in a small applied electric field. J. Cell Sci. **98**:497–506.
28. **McGillivray, A. M., and N. A. R. Gow.** 1986. Applied electrical fields polarize the growth of mycelial fungi. J. Gen. Microbiol. **132**:2515–2525.
29. **McLaughlin, S., and M.-M. Poo.** 1981. The role of electro-osmosis in the electric-field-induced movement of charged macromolecules on the surfaces of cells. Biophys. J. **34**:85–93.
30. **Nanninga, N.** 1991. Cell division and peptidoglycan assembly in *Escherichia coli*. Mol. Microbiol. **5**:791–795.
31. **Niki, H., A. Jaffé, R. Imamura, T. Ogura, and S. Hiraga.** 1991. The new gene *mukB* codes for a 177 kd protein with coiled-coil domains involved in chromosome partitioning of *Escherichia coli*. EMBO J. **10**:183–193.
32. **Nuccitelli, R.** 1990. Vibrating probe technique for studies of ion transport, p. 273–310. *In* J. K. Foskett and S. Grinstein (ed.), Noninvasive techniques in cell biology. Wiley-Liss, Inc., New York.
33. **Poo, M.-M.** 1981. *In situ* electrophoresis of membrane components. Annu. Rev. Biophys. Bioenerg. **10**:245–276.
34. **Poo, M.-M., and K. R. Robinson.** 1977. Electrophoresis of concanavalin A receptors along embryonic muscle cell membrane. Nature (London) **265**:602–605.

34a. **Rajnicek, A. M., C. D. McCaig, and N. A. R. Gow.** Unpublished data.

35. **Richard, C.** 1984. Genus VI. *Enterobacter*, p. 465–469. *In* N. R. Krieg and J. G. Holt (ed.), Bergey's manual of systematic bacteriology. The Williams & Wilkins Co., Baltimore.
36. **Robinson, K. R.** 1985. The responses of cells to electrical fields: a review. J. Cell Biol. **101**:2023–2027.
37. **Robinson, K. R.** 1989. Endogenous and applied electrical currents: their measurement and application, p. 1–25. *In* R. Borgens et al. (ed.), Electric fields in vertebrate repair. Alan R. Liss, Inc., New York.
38. **Rolinson, G. N.** 1980. Effect of β-lactam antibiotics on bacterial cell growth rate. J. Gen. Microbiol. **120**:317–323.
39. **Schwarz, U., A. Asmus, and H. Frank.** 1969. Autolytic enzymes and cell division of *Escherichia coli*. J. Mol. Biol. **41**:419–429.
40. **Spratt, B. G.** 1975. Distinct penicillin binding proteins involved in the division, elongation and shape of *Escherichia coli* K12. Proc. Natl. Acad. Sci. **72**:2999–3003.
41. **Sherwood, J., N. A. R. Gow, G. W. Gooday, D. W. Gregory, and D. Marshall.** 1992. Contact sensing in *Candida albicans*: a possible aid to epithelial penetration. J. Med. Vet. Mycol. **30**:461–469.
42. **Staebell, M., and D. R. Soll.** 1985. Temporal and spatial differences in cell wall expansion during bud and mycelium formation in *Candida albicans*. J. Gen. Microbiol. **131**:1467–1480.